Supporting Information

An inner-filter-effect based ratiometric fluorescent sensor for the detection of uranyl ions in real samples

Hua-Rui Nan [a,b], Yun-Hai Liu [a,c*1], Wen-Juan Gong [a,b], Hong-Bo Peng [a,b], You-Qun Wang [a,c,d], Zhi-Bin Zhang [a,c,d], Xiao-Hong Cao [a,c*1]

[a] State Key Laboratory of Nuclear Resources and Environment, East China University of Technology, Nanchang 330013 Jiangxi, China;

[b]Jiangxi Province Key Laboratory of Synthetic Chemistry, East China University of Technology, Nanchang, Jiangxi 330013, P.R. China

[c] Engineering Research Center of Nuclear Technology Application, East China University of Technology, Nanchang 330013 Jiangxi, China;

[d] Fundamental Science on Radioactive Geology and Exploration Technology Laboratory, East China University of Technology, Nanchang 330013 Jiangxi, China

***Corresponding Authors:** yhliu@ecit.cn (Yunhai Liu); xhcao@ecit.cn (Xiaohong Cao)

[1] Corresponding author. Tel.: +86 791 83897791.
E-mail address: yhliu@ecut.edu.cn (Yunhai Liu); xhcao@ecut.edu.cn (Xiaohong Cao)

Relative fluorescence quantum yield measurement

The relative fluorescence quantum yields (QY) of both B-CDs and AuNCs were calculated according to the method has been reported. Quinine sulfate was used as a reference standard with a quantum yield of 54% (λ_{ex}=360nm). The fluorescence emission spectrums and absorbance at this excitation wavelength (A<0.1) of six sets of solutions with different concentrations of quinine sulfate, B-CDs, and AuNCs were determined. The fluorescence integrated intensities were calculated from the fluorescence emission spectrums. Nitrogen was passed into the solution before measurement to remove dissolved oxygen from the solution to eliminate the quench of the oxygen to fluorescence. The formula used for QY measurement is as follows:

$$Q_x = Q_s\left(\frac{\eta_x^2}{\eta_s^2}\right)\left(\frac{A_s}{A_x}\right)\left(\frac{F_x}{F_s}\right) \qquad (1)$$

where Q is the quantum yield, η is refractive index of the solvent, F is the area integral of the emission spectrum, A refers the absorbance at excitation wavelength. Quinine sulfate was dissolved in 0.1 M H_2SO_4 (η=1.33) and the B-CDs and AuNCs were dissolved in ultrapure water (η=1.33). "S" and "X" represent standard reference and sample. According to above equation, QY of B-CDs and AuNCs were determined to be 42.2% and 21.6%, separately.

The modified Parker model

$$\frac{F_{corr}}{F_{obs}} = \frac{2.3dA_{\lambda ex}}{1-10^{-dA_{\lambda ex}}} \times 10^{gA_{\lambda em}} \times \frac{2.3sA_{\lambda em}}{1-10^{-sA_{\lambda em}}} \qquad (2)$$

In this equation, the correction factor (CF) was calculated by F_{corr}/F_{obs}; F_{obs} is the observed fluorescence intensity; F_{corr} is the corrected fluorescence intensity after removing IFE from F_{obs}.; $A_{\lambda ex}$ and $A_{\lambda em}$ refer to the absorbance of the solution at the excitation (365 nm) and emission (676 nm) wavelengths, separately; *s* is the width of the excitation light; *d* is the width of the cuvette cell; *g* is the distance from the edge of

the excitation beam to the edge of the cuvette cell. The calibration results are reliable when the maximum value of the correction factor does not exceed 3.

The correction experiments of IFE

In a typical correction experiment, different concentrations of uranyl ions and 100 μL of AuNPs were added into quartz cuvette. Next, 200 μL of AuNCs solution were added into the cuvette. Finally, the Britton-Robinson buffer of pH 2.5 was added to the dispersion with a total volume of the solution of 4.0 mL and incubated at 25 ℃ for 12min. The absorbance of the mixture at 365nm and 676nm were collected by UV–vis spectrometer, and the fluorescence intensity of AuNCs was measured.

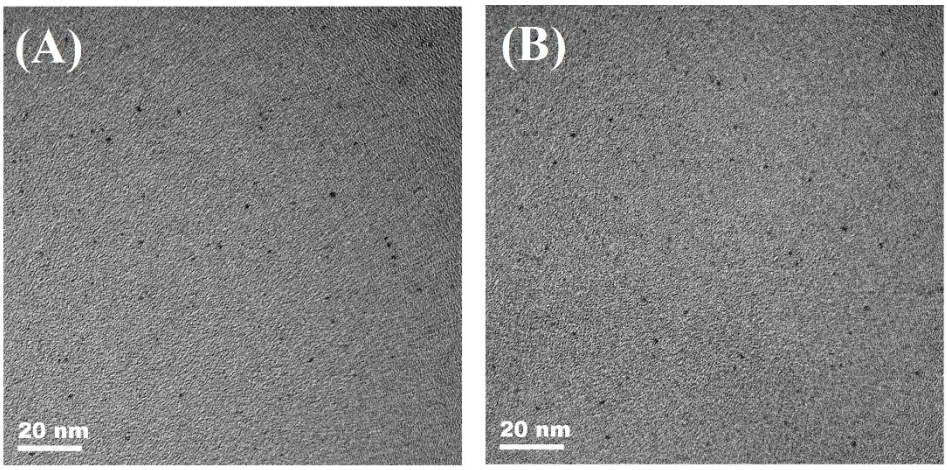

Fig. S1 TEM images of B-CDs(A), AuNCs(B),

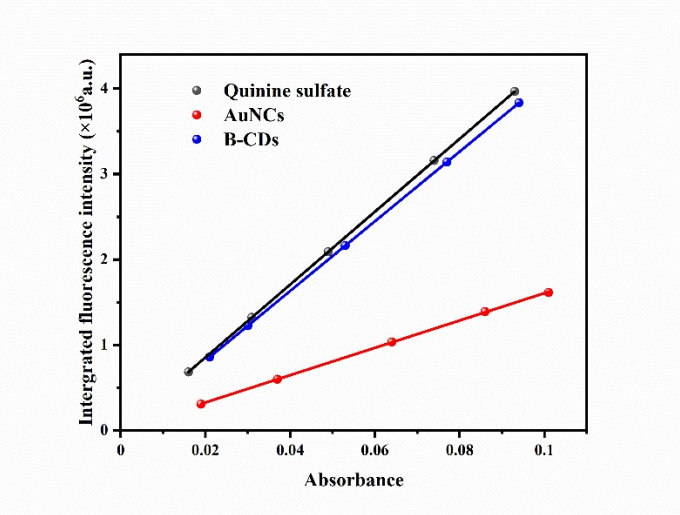

Fig. S2 The relative quantum yield of B-CDs and AuNCs.

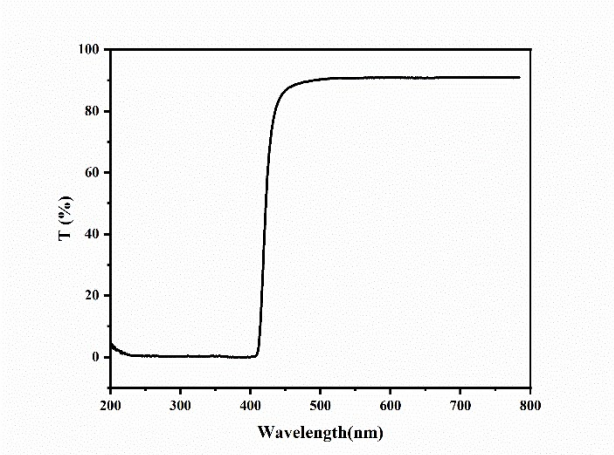

Fig. S3 The transmittance of filter L-42 in the range of 200-800nm.

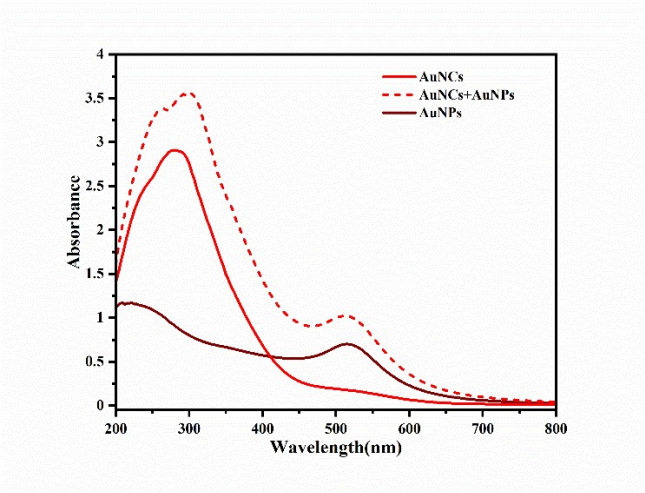

Fig S4 The UV-vis spectrums of AuNCs before and after the addition of dispersed AuNPs.

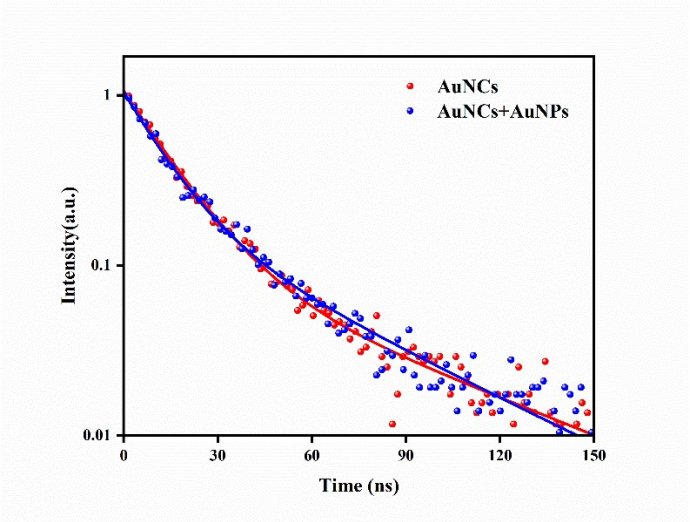

Fig S5 Fluorescence decay plots of AuNCs in the absence (red) and presence (blue) of AuNPs.

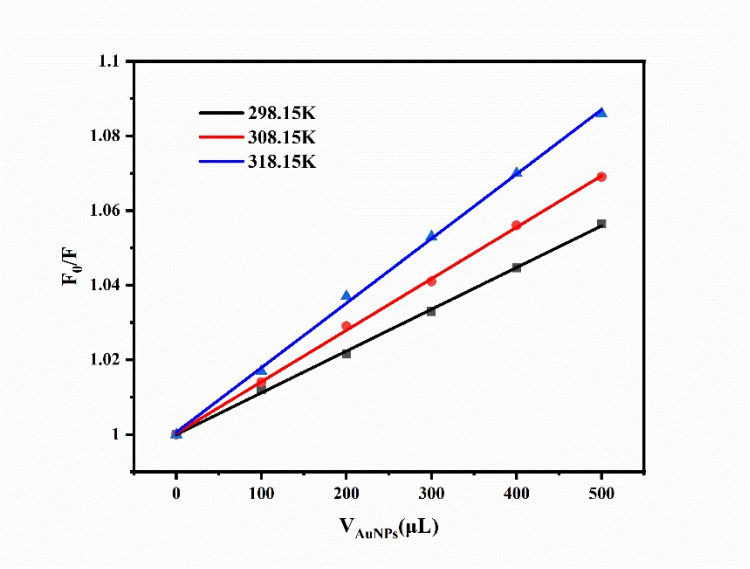

Fig S6 The Stern-Volmer plot in different temperature.

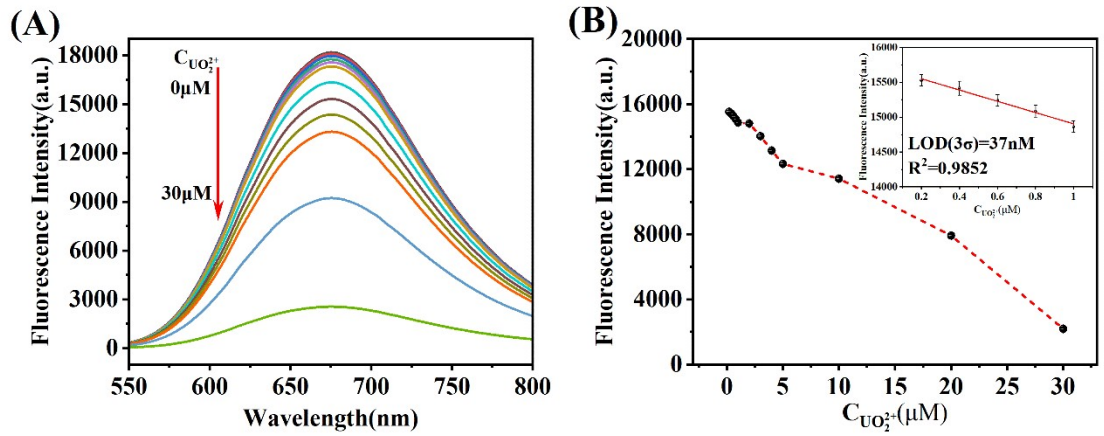

Fig S7 (A) The fluorescence spectrums of the single-signal fluorescent sensing system after the addition of different concentrations of uranyl ions. inset: The corresponding fluorescence intensity changes under 365 nm UV illumination. (B) The relationship between the intensity of fluorescence at 676nm and the concentration of uranyl ions. inset: The linear relationship of intensity and the concentration of uranyl ions in the range of from 0.2 μmol/L to 1.0 μmol/L.

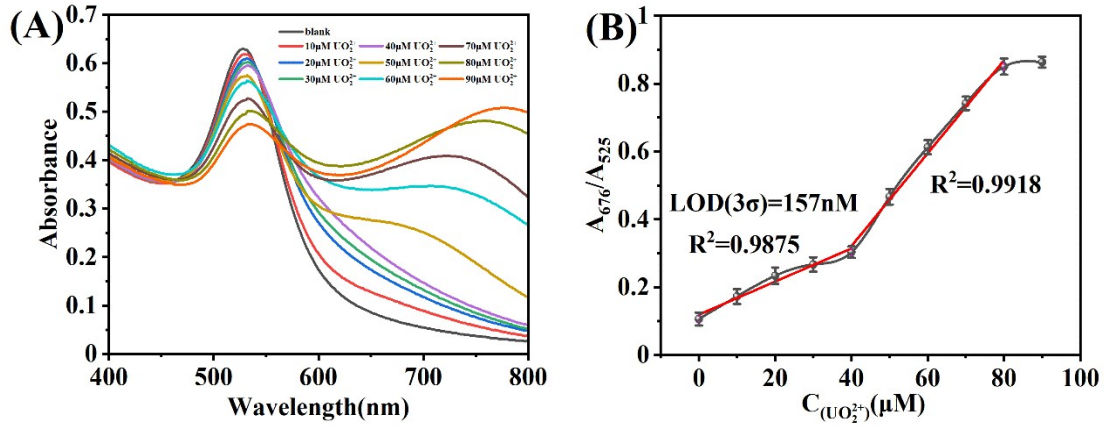

Fig S8 (A) The adsorption spectrums of the AuNPs after the addition of different concentrations of uranyl ions. inset: The corresponding color changes under natural light. (B) The relationship between the ratio of absorbance A_{676}/A_{520} and the concentration of uranyl ions.

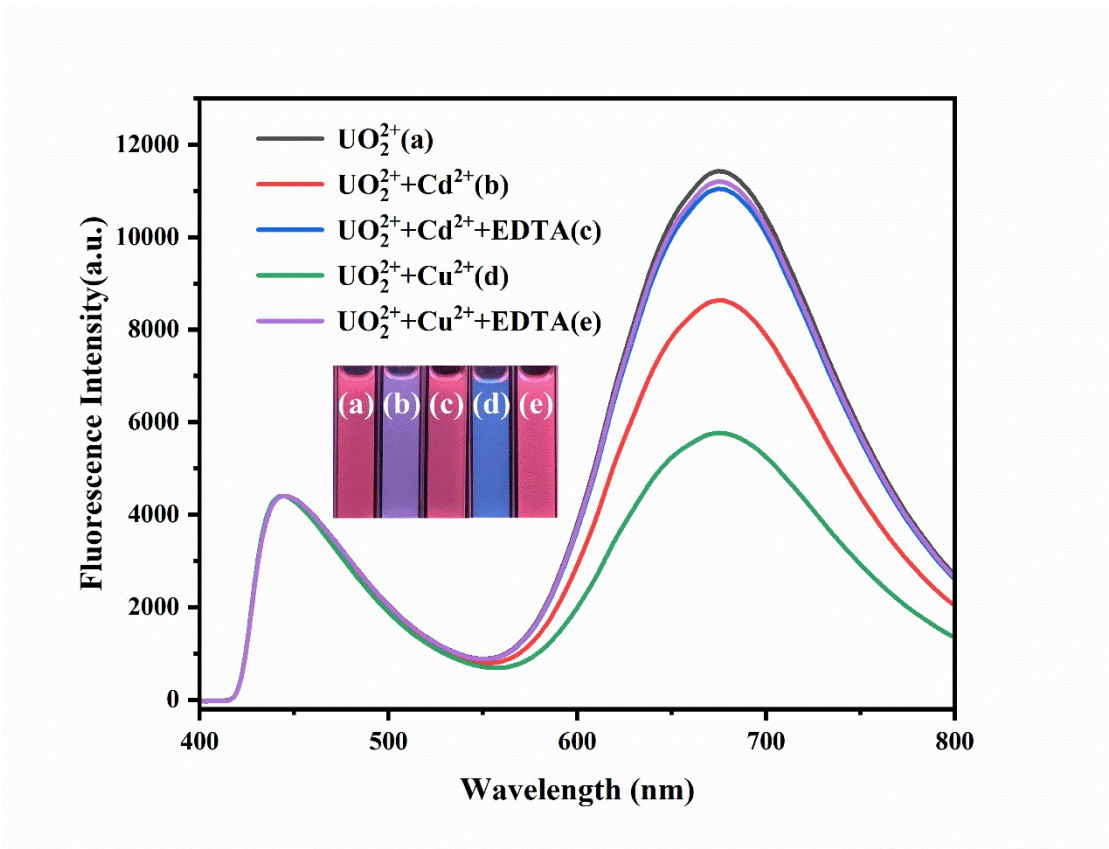

Fig S9 Elimination of Cd^{2+} or Cu^{2+} (250 μM) interference in the presence of EDTA (1 mM).

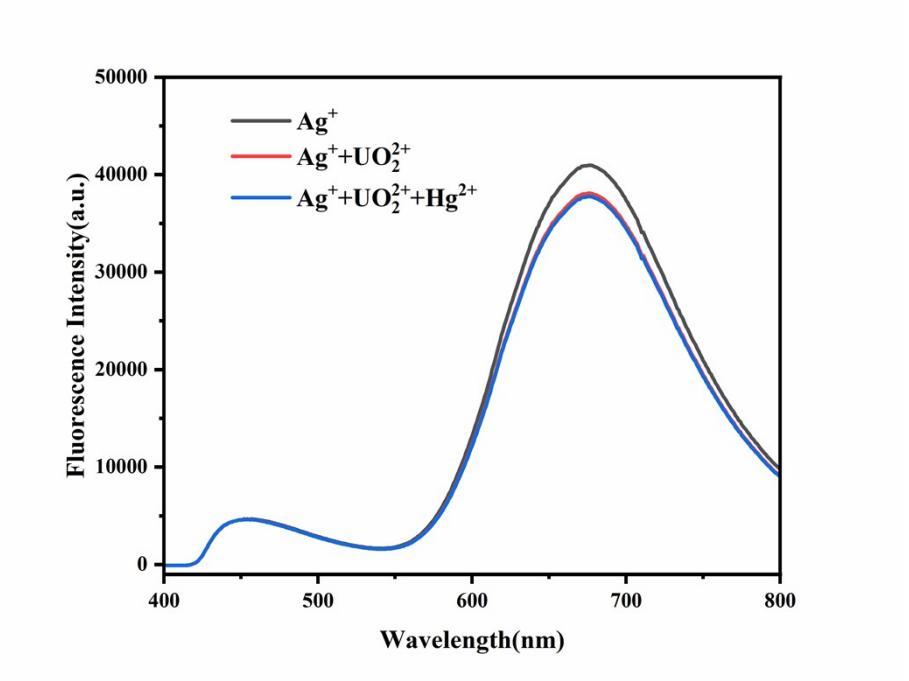

Fig S10 Elimination of Hg^{2+} interference in the presence of Ag^+ ions (10 μM). The concentrations of Hg^{2+} and UO_2^{2+} are all 5 μM.

Table S1 A comparison of present work with other fluorescent probes for UO_2^{2+} sensing

Probes	Mechanisms	LOD ($nmol \cdot L^{-1}$)	Ref
HFSA	Ratiometric, AIE	1.9	[1]
TPE-T	Single-signal, AIE	-	[2]
PCSA	Single-signal, AIE	0.7	[3]
APIDCE	Single-signal, PET	10	[4]
TCPP-PNIPAM	Single-signal, FRET	1.1	[5]
CdS-MAA	Single-signal, ET	0.3	[6]
B-CDs&R-CDs	Ratiometric, ET	8.15×10^3	[7]
C-dots&CdTe QDs	Ratiometric, ET	5×10^2	[8]
B-CDs&AuNCs	Ratiometric, IFE	8.4	This Work
AuNCs	Single-signal, IFE	37	This Work

AIE: aggregation-induced emission; PET: photoinduced electron transfer; ET: electron transfer.

Table S2 Concentration of different ions of the solution in the evaporation cell

pH	UO_2^{2+}(μM)	HCO_3^- (mM)	Ca^{2+}(mM)	Mg^{2+}(mM)	SO_4^{2-}(mM)	Cl^-(mM)
1.13	588.32	18.52	5.02	6.33	19.45	0.37

References

1. Chen, X.; Peng, L.; Feng, M.; Xiang, Y.; Tong, A.; He, L.; Liu, B.; Tang, Y., An aggregation induced emission enhancement-based ratiometric fluorescent sensor for detecting trace uranyl ion (UO_2^{2+}) and the application in living cells imaging. *Journal of Luminescence* **2017,** *186*, 301-306.

2. Wen, J.; Huang, Z.; Hu, S.; Li, S.; Li, W.; Wang, X., Aggregation-induced emission active tetraphenylethene-based sensor for uranyl ion detection. *J Hazard Mater* **2016,** *318*, 363-370.

3. Chen, X.; He, L.; Wang, Y.; Liu, B.; Tang, Y., Trace analysis of uranyl ion (UO_2^{2+}) in aqueous solution by fluorescence turn-on detection via aggregation induced emission enhancement effect. *Anal Chim Acta* **2014,** *847*, 55-60.

4. Ma, J.; He, W.; Han, X.; Hua, D., Amidoximated fluorescent polymer based sensor for detection of trace uranyl ion in aqueous solution. *Talanta* **2017,** *168*, 10-15.

5. Shu, X.; Wang, Y.; Zhang, S.; Huang, L.; Wang, S.; Hua, D., Determination of trace uranyl ion by thermoresponsive porphyrin-terminated polymeric sensor. *Talanta* **2015,** *131*, 198-204.

6. Dutta, R. K.; Kumar, A., Highly Sensitive and Selective Method for Detecting Ultratrace Levels of Aqueous Uranyl Ions by Strongly Photoluminescent-Responsive Amine-Modified Cadmium Sulfide Quantum Dots. *Anal Chem* **2016,** *88* (18), 9071-9078.

7. Qian, J.; Cao, N.; Zhang, J.; Hou, J.; Chen, Q.; Zhang, C.; Sun, Y.; Liu, S.; He, L.; Zhang, K.; Zhou, H., Field-portable ratiometric fluorescence imaging of dual-color label-free carbon dots for uranyl ions detection with cellphone-based optical platform. *Chinese Chemical Letters* **2020,** *31* (11), 2925-2928.

8. Chen, X.; Mei, Q.; Yu, L.; Ge, H.; Yue, J.; Zhang, K.; Hayat, T.; Alsaedi, A.; Wang, S., Rapid and On-Site Detection of Uranyl Ions via Ratiometric Fluorescence Signals Based on a Smartphone Platform. *ACS Appl Mater Interfaces* **2018,** *10* (49), 42225-42232.